International Journal of Control, Automation and Systems 16(6) (2018) 3047-3054
http://dx.doi.org/10.1007/s12555-018-0179-6
ISSN:1598-6446 eISSN:2005-4092
http://www.springer.com/12555

Temperature Control of a Regasification System for LNG-fuelled Marine Engines Using Nonlinear Control Techniques

Gun-Baek So, Hyun-Sik Yi, Yung-Deug Son, and Gang-Gyoo Jin*

Abstract: This paper presents two nonlinear PID (NPID) controllers which control the glycol temperature of a regasification system for LNG-fuelled engines. The NPID controllers have a parallel structure of the three nonlinear P, I, D actions or the linear P, D actions and nonlinear I action. A nonlinear function is employed to scale the error as input of the integral and implemented as a Takagi-Sugeno (T-S) fuzzy model. The controller parameters are optimally tuned by using a genetic algorithm. Furthermore, the stability problem of the overall system is verified based on the circle criterion. A set of simulation works is carried out to validate the efficiency of the two proposed controllers.

Keywords: Circle criterion, nonlinear PID controller, temperature control, T-S fuzzy model.

1. INTRODUCTION

Excessive use of fossil fuels resources is adding several types of greenhouse gases which make the Earth warmer. Emissions from ship's exhausts contribute to global climate change, too. The International Maritime Organization (IMO) has adopted regulations to reduce the emission of air pollutants from international shipping, such as carbon dioxide (CO_2), nitrogen oxides (NOx), and sulphur oxides (SOx) under Annex VI of the 1997 MARPOL protocol [1, 2].

Meanwhile, large engine manufacturers, such as MAN B&W and Wartsila, have been developing LNG-fuelled engines [3, 4]. The use of liquefied natural gas (LNG) requires special equipments which can handle cryogenic temperatures (-162°C) and designing technologies of high-pressure dual fuel (HPDF) engines. HPDF engines work on diesel cycle in gas mode. To use cryogenic LNG as fuel, it has to be converted to gas at around 30-50°C, and this process is called LNG regasification.

Recently some studies have been done to control the temperature of shell-tube type heat exchangers. Vinaya *et al*. [5] proposed a discrete model predictive control algorithm, and Pandey *et al*. [6] proposed a PI-type fuzzy controller. Sivakumar *et al*. [7] investigated a method of combining neurofuzzy control with the PID control technique, and Sarabeevi *et al*. [8] addressed the problem associated with using a PID controller based on an internal model.

However, many industrial processes are highly nonlinear and their parameters change during operation. Although a fixed-gain controller is effective in a limited operating range, its performance degrades and may become unstable in some cases when it is out of this range. This problem can be solved, to some extent, by introducing nonlinear elements in the PID control structure. Some forms of nonlinear PID controllers have been studied for industrial processes. They can be categorized into two types. One is the nonlinear PID controller introduced by Korkmaz *et al*. [9] and Isayed [10], whose gains are gradually changed based on error and/or error rate. The other is the nonlinear PID controller introduced by Seraji [11] and Zaidner *et al*. [12], where a nonlinear gain in cascade with a linear PID controller produces the scaled error. The former makes it difficult to analyze the stability by using three nonlinear gains and the latter has the disadvantage of using a single nonlinear gain without consideration of the characteristics of the three actions.

This paper presents two nonlinear PID controllers which control the outlet temperature of glycol on the secondary loop of a regasification system for LNG-fuelled engines. The nonlinear PID controllers combine the three nonlinear P, I, D actions or the linear P, D actions and nonlinear I action. A nonlinear function, employed to scale

Manuscript received March 22, 2018; revised June 18, 2018; accepted July 20, 2018. Recommended by Associate Editor Jong Min Lee under the direction of Editor Jay H. Lee.

Gun-Baek So is with the Department of Convergence Study on the OST, OST School, KMOU, 727 Taejong-ro, Yeongdo-gu, Busan, Korea (e-mail: superior3608@naver.com). Hyun-Sik Yi is with Lynx Computing Systems Inc., #302 39 Jijokbuk-ro, Yuseong, Daejeon 34070, Korea (e-mail: hyunsik.yi@ilynxsys.com). Yung-Deug Son is with Department of Mechanical Facility Control Engineering, Korea University of Technology and Education, 1600 Chungjeol-ro, Dongnam-gu, Cheonan-si, Chungcheongnam-do, Korea (ydson@koreatech.ac.kr). Gang-Gyoo Jin is with the Division of Control and Automation Engineering, KMOU, 727 Taejong-ro, Yeongdo-gu, Busan, Korea (e-mail: ggjin@kmou.ac.kr).
* Corresponding author.

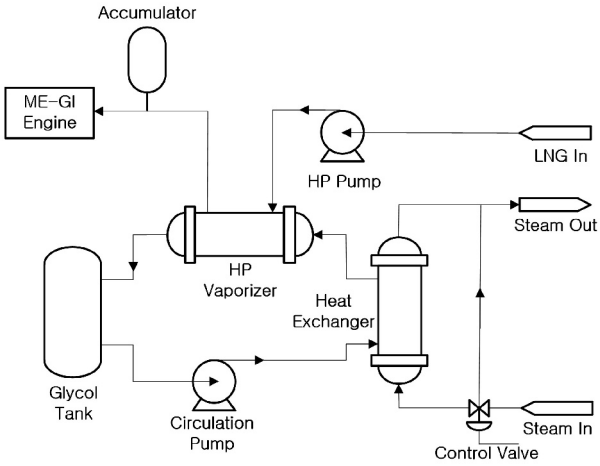

Fig. 1. A regasification system for LNG-fuelled marine engines.

the error, is described by a Takagi-Sugeno (T-S) fuzzy model. The parameters of the proposed controllers are tuned by a genetic algorithm (GA) from the viewpoint of minimizing the integral of absolute error (IAE) performance index. Since the introduction of a nonlinear function causes the stability problem of the feedback system, it is analyzed using the circle criterion. To validate the effectiveness of the proposed methods, a set of simulation works are performed.

2. A HEAT EXCHANGE SYSTEM

A regasification system for LNG-fuelled marine engines is shown in Fig. 1.

The regasification system is divided into the primary and secondary loops. After pumping cryogenic LNG on the primary loop to approximately 250-300 bar, it is heated in a high-pressure vaporizer to the gas state of 30-50°C and this gas is then fed to the engine cylinder through an injector. When LNG is vaporizing, it receives thermal energy from glycol as an intermediate heating medium. Meanwhile, on the secondary loop, the glycol cooled down in the vaporizer is reheated by hot steam supplied to the heat exchanger.

The objective of the proposed control schemes is to maintain the outlet temperature of glycol by controlling the amount of steam supplied to the heat exchanger on the secondary loop. The transfer function of each subsystem can be expressed as follows [7, 8]:

I/P converter and diaphragm valve

$$G_v(s) = \frac{K_{ip}K_v}{1+T_v s}, \tag{1}$$

heat exchanger

$$G_h(s) = \frac{K_h}{1+T_h s}, \tag{2}$$

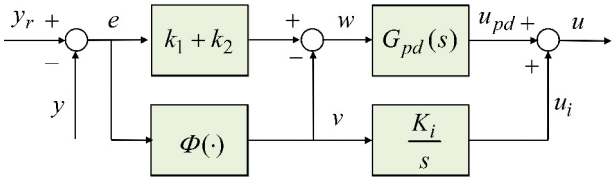

Fig. 2. The proposed F-NPID controller.

disturbance

$$G_d(s) = \frac{K_{dis}}{1+T_h s}, \tag{3}$$

measurement sensor

$$H(s) = \frac{K_s}{1+T_s s}, \tag{4}$$

where K_{ip}, K_v, and T_v are the constant of the I/P converter (psi/mA), the gain (kg/sec·psi) and time constant (sec) of the diaphragm valve, respectively; K_h and T_h the gain (°C·sec/kg), the time constant (sec) of the heat exchanger; K_{dis} the gain of the disturbance model; K_s and T_s the gain (mA/°C) and the time constant (sec) of the measurement sensor, respectively.

3. CONTROLLER DESIGN

The proportional action grows or shrinks in proportion to the error e. If a large proportional gain is maintained even for a small error, excessive control can cause overshoot and oscillation. The derivative action also increases or decreases in proportion to the error rate. If a large derivative gain is kept even for a small error, control can be sensitive to noise. Therefore, e should be properly reduced when the response reaches around the set–point. Once a large change in set-point occurs or a large disturbance applies, the integral of the error keeps increasing fast and overshoot occurs. When the error is so small, the integral action is still collecting error until it is large enough to eliminate the steady-state error completely. The integral of the error should be small action when the error is large, and large when the error is small to avoid overshoot and to remove offset quickly. Thus, the integral action should be different depending on the size of the error. This can be dealt by introducing a nonlinear function.

According to this fact, we propose two nonlinear PID controllers that can give satisfactory response for the glycol temperature control of the heat exchanger.

3.1. The fully-nonlinear PID controller

One forms a combination of the nonlinear P, I, D actions as shown in Fig. 2. Hereafter, this is called the fully-nonlinear PID (F-NPID) controller. In Fig. 2, y_r, y, and u denote the reference input, measured output, and control input, respectively; e the error which is defined as $e =$

$y_r - y$; u_{pd} and u_i the outputs of the PD action and I action, respectively.

The nonlinear PD action with a first-order filter is expressed by

$$w(t) = (k_1 + k_2)e(t) - v(t), \tag{5a}$$
$$v(t) = \Phi(e) = k(e)e(t), \tag{5b}$$
$$T_f \dot{u}_d(t) + u_d(t) = K_d \dot{w}(t), \tag{5c}$$
$$u_{pd}(t) = K_p w(t) + u_d(t), \tag{5d}$$

where u_d is the derivative action; K_p and K_d the proportional and derivative gains, respectively; $T_f = K_d/(NK_p)$ the filter time constant; and the maximum derivative gain N is an empirically determined constant and $N = 10$ is used [14]. $k(e)$ is a nonlinear gain, $\Phi(e)$ a nonlinear function which provides a nonlinearly-scaled error according to e, and $v(t)$ a scaled error.

By using a Takagi-Sugeno (T-S) fuzzy model [15] as a nonlinear function, those preferred actions described before are possible. $\Phi(e)$ has the following form:

$$R_1: \text{ if } e \text{ is } F_1, \text{ then } \Phi(e) = k_1 e, \tag{6a}$$
$$R_2: \text{ if } e \text{ is } F_2, \text{ then } \Phi(e) = k_2 e, \tag{6b}$$
$$R_3: \text{ if } e \text{ is } F_3, \text{ then } \Phi(e) = k_1 e, \tag{6c}$$

where e is linguistic variable representing the error as an input of the fuzzy system, F_i $(i = 1, 2, 3)$ fuzzy sets defined on e, and k_1 and k_2 are user-defined positive constants $(0 \leq k_1 < k_2)$. Meanwhile, the membership functions of F_1, F_2, and F_3 are given by (7)-(9):

$$F_1(e) = \begin{cases} 1, & e \leq -3\sigma, \\ -e/3\sigma, & -3\sigma < e \leq 0, \\ 0, & \text{elsewhere}, \end{cases} \tag{7}$$

$$F_2(e) = \exp\left(-\frac{e^2}{2\sigma^2}\right), \tag{8}$$

$$F_3(e) = \begin{cases} e/3\sigma, & 0 \leq e < 3\sigma, \\ 1, & e \geq 3\sigma, \\ 0, & \text{elsewhere}, \end{cases} \tag{9}$$

where σ is the standard deviation of $F_2(e)$ and a user-defined parameter. When the fuzzy sets are defined, they are overlapped such that $\sum_{i=1}^{3} \alpha_i > 0$ is always true for all e.

Given the input e, the final output $\Phi(e)$ of the fuzzy system is inferred by

$$\Phi(e) = (\alpha_1 k_1 + \alpha_2 k_2 + \alpha_3 k_1)e/(\alpha_1 + \alpha_2 + \alpha_3), \tag{10}$$

where the weight α_i implies the membership grade of e in $F_i(e)$. The shape of $\Phi(e)$ depends on k_1, k_2 and σ. Fig. 3 shows a graphic interpretation of the T-S fuzzy inference system for a typical fuzzy singleton input e_0.

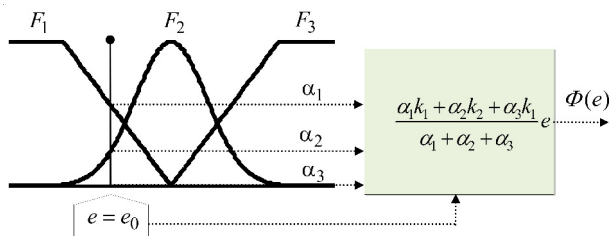

Fig. 3. The T-S fuzzy inference system for obtaining $\Phi(e)$.

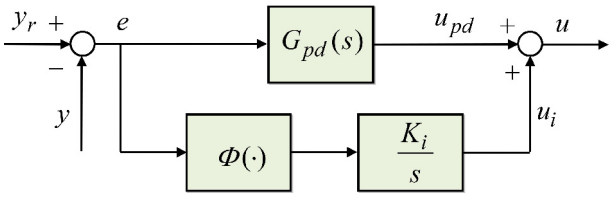

Fig. 4. The proposed P-NPID controller.

The transfer function of the linear part from $w(t)$ to $u_{pd}(t)$ yields

$$G_{pd}(s) = \frac{U_{pd}(s)}{W(s)} = K_p + \frac{K_d s}{1 + T_f s}. \tag{11}$$

For the nonlinear integral action, (12) is employed:

$$u_i(t) = K_i \int v(t)dt, \tag{12}$$

where K_i is the integral gain.

3.2. The partially-nonlinear PID controller

As can be seen in the previous subsection, the F-NPID controller has 5 tuning parameters (K_p, K_i, K_d, k_1 and σ) if k_2 is fixed to 1 later, so the degree of freedom is increased rather than the conventional PID controller, but tuning may be a burden. Focusing on the fact that the proportional and derivative actions are static systems, but the integral action is a dynamic system in which previous errors are accumulated, the other controller employs the the integral action in cascade with the nonlinearity $\Phi(e)$ incorporating the linear P, D actions. On the other hand, k_1 and k_2 are set to 0 and 1, respectively. Hereafter, this is called the partially-nonlinear PID (P-NPID) controller. Fig. 4 shows its simplified structure. In Fig. 4, $\Phi(e)$ is the same function used in (6).

The overall block diagram that combines one of the proposed controllers with the plant is depicted in Fig. 5.

3.3. Tuning of the NPID controllers

Controller tuning is a process of determining the NPID parameters which generate the desired output. The NPID controllers are off-linely tuned by a real-coded genetic algorithm, hereafter called RCGA.

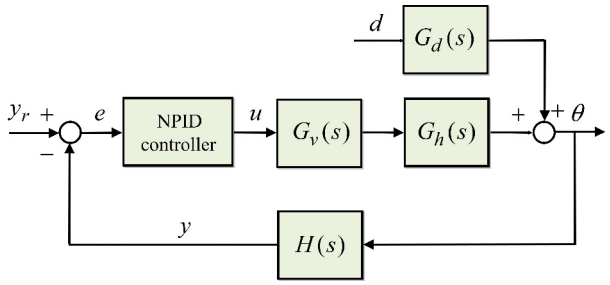

Fig. 5. Overall feedback control system.

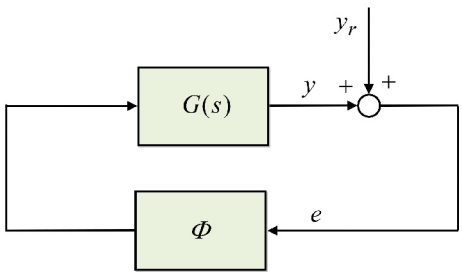

Fig. 6. Equivalent feedback control system.

The RCGA processes a population of vectors of real numbers which represent the parameters of the NPID controllers. Arithmetical crossover and non-uniform mutation [17] are used for crossover and mutation operators, respectively. The RCGA starts off with a population of randomly generated real vectors. In order to obtain the optimal parameter set which gives satisfactory response, the population is evaluated by minimizing one of the following IAE criteria:

$$J(K_p,K_i,K_d,\alpha,k_1)=\int_0^{t_f}|e(t)|dt, \tag{13a}$$

$$J(K_p,K_i,K_d,\alpha)=\int_0^{t_f}|e(t)|dt, \tag{13b}$$

where t_f is a sufficiently large time.

4. STABILITY ANALYSIS

In this section, circle stability theory is applied for the stability analysis of nonlinear systems. The nonlinear system in Fig. 5 can be decomposed into a linear block $G(s)$ and a nonlinear block Φ as shown in Fig. 6. Here, y_r is considered as constant or zero and disturbance d as zero for convenience.

The linear transfer function $G(s)$ in the case of the F-PID controller is then

$$\begin{aligned}G(s)&=\frac{G_v(s)G_h(s)H(s)[K_i-sG_{pd}(s)]}{s[1+(k_1+k_2)G_{pd}(s)G_v(s)G_h(s)H(s)]}\\&=\frac{N_F(s)}{D_F(s)},\end{aligned} \tag{14}$$

where $N_F(s)=G_v(s)G_h(s)H(s)[K_i-sG_{pd}(s)]$, $D_F(s)=s[1+(k_1+k_2)G_{pd}(s)G_v(s)G_h(s)H(s)]$ and $\deg(N_F(s))<\deg(D_F(s))$.

And $G(s)$ in the case of the P-PID controller is

$$\begin{aligned}G(s)&=\frac{K_iG_v(s)G_h(s)H(s)}{s[1+G_{pd}(s)G_v(s)G_h(s)H(s)]}\\&=\frac{N_P(s)}{D_P(s)},\end{aligned} \tag{15}$$

where $N_P(s)=K_iG_v(s)G_h(s)H(s)$, $D_P(s)=s[1+G_{pd}(s)G_v(s)G_h(s)H(s)]$ and $\deg(N_P(s))<\deg(D_P(s))$.

Definition 1: A memoryless function $\Phi:\Re\to\Re$ is said to belong to the sector $[k_1,k_2]$, if there exist two non-negative numbers k_1 and k_2 ($k_2>k_1$) such that

$$k_1e\le\Phi\le k_2e,\quad\forall e\in\Re. \tag{16}$$

In (16), $\Phi(0)=0$ and the relationship of $\Phi\cdot e\ge 0$ is always true. Geometrically, $\Phi\in[k_1,k_2]$ exists between the two straight lines k_1e and k_2e, that is, it exists in the first and third quadrants, as shown in Fig. 6.

Theorem 1: Consider the T-S fuzzy system in (6). If $0\le k_1<k_2$, then the mapping of the T-S fuzzy system $\Phi(e)$ belongs to the sector $[k_1,k_2]$.

Proof: From the result of the fuzzy inference in (10) and the fact that $\alpha_1+\alpha_2+\alpha_3\neq 0$, clearly we have

$$\Phi(e)\ge\frac{\alpha_1k_1+\alpha_2k_1+\alpha_3k_1}{\alpha_1+\alpha_2+\alpha_3}e=k_1e,$$

and also

$$\Phi(e)\le\frac{\alpha_1k_2+\alpha_2k_2+\alpha_3k_2}{\alpha_1+\alpha_2+\alpha_3}e=k_2e.$$

Since we have $k_1e\le\Phi(e)\le k_2e$, hence $\Phi(e)\in[k_1,k_2]$. □

As typical cases, if k_2 is set to 1 for the F-NPID controller, $\Phi(e)\in[k_1,1]$, and if k_1 and k_2 are set to 0 and 1, respectively for the P-NPID controller, $\Phi(e)\in[0,1]$.

Theorem 2: Consider the feedback system in Fig. 6 where $G(s)$ is stable (i.e., it has all its poles in the left half-plane with one pole at the origin) and $\Phi\in[k_1,k_2]$, $k_1<k_2$. Then, the system is absolutely stable if the following condition is satisfied:

$$\mathrm{Re}\left[\frac{1+k_2G(j\omega)}{1+k_1G(j\omega)}\right]>0,\quad\omega\in\Re. \tag{17}$$

Proof: Theorem 2 can be proved by using loop transformation, a Lyapunov function and the Kalman-Yakubovich-Popov equations. See [16].

Lemma 1: Consider the system in Fig. 6 where $G(s)$ is stable and $\Phi\in[k_1,k_2]$. Then, the system is absolutely stable if one of the following conditions is satisfied:

1) If $0<k_1<k_2$, then the Nyquist plot of $G(j\omega)$ does not penetrate the disk $D(k_1,k_2)$ having as diameter the segment $[-1/k_1,-1/k_2]$ located on the x-axis.

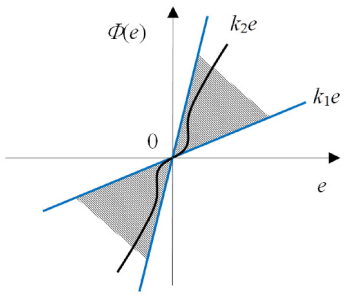

Fig. 7. Geometrical representation of the sector $[k_1, k_2]$.

2) If $0 = k_1 < k_2$, then the Nyquist plot of $G(j\omega)$ is located on the right of a vertical line defined by $\mathrm{Re}(s) = -1/k_2$.

Proof: Suppose that $G(j\omega) = u + jv$. In the case of $0 < k_1 < k_2$, equation (17) can be rewritten as:

$$Re\left[\frac{1/k_2 + G(j\omega)}{1/k_1 + G(j\omega)}\right] = \frac{(1/k_2+u)(1/k_1+u)+v^2}{(1/k_1+u)^2+v^2} > 0.$$

Rearranging the above inequality with the fact that the denominator is never zero yields

$$[u + \frac{1}{2}(\frac{1}{k_1}+\frac{1}{k_2})]^2 + v^2 > [\frac{1}{2}(\frac{1}{k_1}-\frac{1}{k_2})]^2.$$

This inequality implies that the Nyquist plot of $G(j\omega)$ locates the outside of the circle with the center of $-0.5(1/k_1 + 1/k_2) + j0$ and a radius $0.5(1/k_1 - 1/k_2)$ and never enter the disk $\mathrm{D}(k_1, k_2)$, shown in Fig. 8(a).

In the case of $0 = k_1 < k_2$, equation (17) can be rewritten as

$$Re\,[1 + k_2 G(j\omega)] = 1 + k_2 u > 0.$$

Rearranging the above inequality yields

$$\mathrm{Re}G(j\omega) = u > -1/k_2.$$

□

This inequality implies that the Nyquist plot of $G(j\omega)$ lies to the right of a vertical line defined by $\mathrm{Re}G(j\omega) = -1/k_2$, shown in Fig. 8(b).

To demonstrate that the F-NPID control system in Fig. 5 is absolutely stable, applying the parameters in Table 1 and Table 2 to (14) gives $N_F(s) = -3.451s^2 - 0.576s + 0.006$ and $D_F(s) = s^5 + 60.243s^4 + 27.943s^3 + 9.397s^2 + 1.157s$. It can be easily verified that $G(s)$ has five stable poles at 0, -59.778, -0.184, and $-0.140 \pm j0.292$. We can apply the first case of Lemma 1.

Clearly, the choice of k_2 may not be unique. The Nyquist plot of $G(j\omega)$ shown in Fig. 9 is on the right of the vertical line $\mathrm{Re}(s) = -0.561$. Therefore, $-1/k_2 = -0.561$, that is, $k_2 = 1.783$. This means that the system is absolutely stable for all values of k_2 less than 1.783.

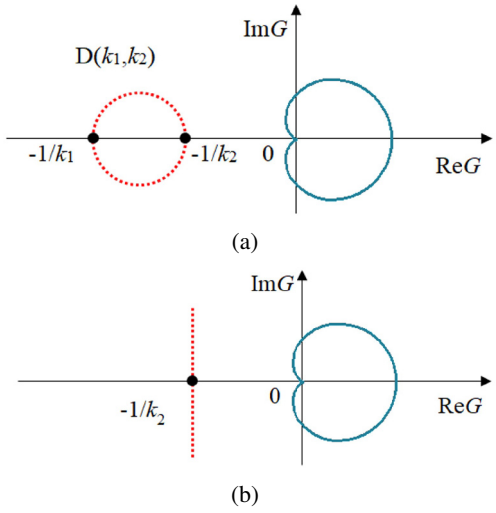

Fig. 8. Disk $\mathrm{D}(k_1, k_2)$ and Nyquist plot of $G(j\omega)$.

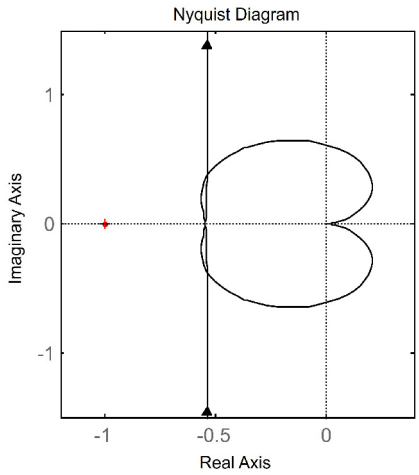

Fig. 9. Nyquist plot of $G(j\omega)$.

Hence, we can conclude that the feedback system is absolutely stable for all nonlinearities $\Phi \in [0.895, 1]$.

In the case of the P-NPID control system in Fig. 6, applying the parameters in Table 1 and Table 2 to (15) gives $N_P(s) = -0.338 \times 10^{-3}s + 0.019$ and $D_P(s) = s^5 + 57.865s^4 + 26.834s^3 + 6.350s^2 + 0.690s$. $G(s)$ have five stable poles at 0, -57.400, -0.212, and $-0.127 \pm j0.202$. We can apply the second case of Lemma 1.

The Nyquist plot of $G(j\omega)$ shown in Fig. 10 is on the right of the vertical line $\mathrm{Re}(s) = -0.255$. Therefore, $-1/k_2 = -0.255$, that is, $k_2 = 3.922$. This means that the system is absolutely stable for all values of k_2 less than 3.922. Hence, we can conclude that the feedback system is absolutely stable for all nonlinearities $\Phi \in [0, 1]$.

5. SIMULATION RESULTS

A set of simulation works are performed to verify the effectiveness of the proposed methods on the plant with

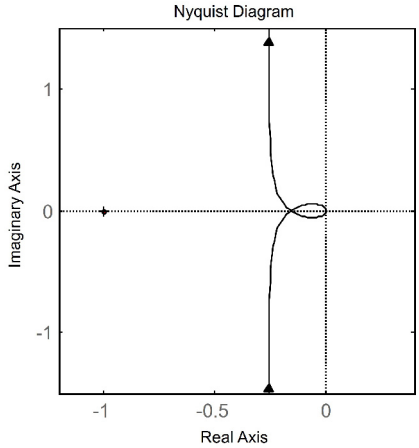

Fig. 10. Nyquist plot of $G(j\omega)$.

Table 1. Parameters of the plant.

Parameter	Value
K_{ip}	0.75 psi/mA
K_v	0.4/3 kg/sec.psi
T_v	3 sec
K_h	12.5 ∘C.sec/kg
T_h	30 sec
K_s	0.2 mA/°C
T_s	10 sec
K_{dis}	1

Table 2. Tuned controller parameters.

Method	Gains			Remarks
	K_p	K_i	K_d	
F-NPID	34.671	0.339	207.249	$\sigma = 0.370, k_1 = 0.895, k_2 = 1$
P-NPID	39.289	1.215	225.502	$\sigma = 0.175, k_1 = 0, k_2 = 1$
S-NPID	46.808	1.336	108.338	$k_0 = 0, k_1 = 1, k_2 = 1$
Z-N	44.882	3.122	161.296	$K_u = 76.3, P_u = 28.8$
T-L	34.682	0.548	158.270	

the parameters in Table 1. The results are then compared with those of the Seraji [14], Ziegler-Nichols (Z-N), and Tyreus-Luyben (T-L) methods. An optimal tuning of the Seraji and proposed NPID controllers are done by a RCGA.

The linear PID controller gains are tuned based on inducing ultimate vibration. The ultimate gain K_u and the ultimate period P_u are 76.3 and 28.8, respectively.

5.1. Response to set-point (SP) change

During warming-up, an operator preheats the coolant, lubricant, and fuel oil to the desired temperatures to prepare the engine for startup. In the case of LNG-fuelled engines, the temperature is gradually increased over time because the liquid LNG must be raised slowly to the normal

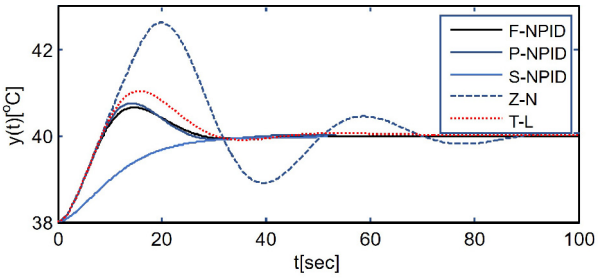

Fig. 11. Responses of the four methods when the SP is step-wisely changed from 38 to 40°C.

Table 3. Quantitative comparison of the SP tracking performance.

Method	SP tracking performance				
	t_r	t_p	M_p	t_s	IAE
F-NPID	5.955	14.750	32.869	38.965	18.327
P-NPID	5.834	14.300	38.113	36.130	18.463
S-NPID	20.598	149.950	0.341	39.524	25.341
Z-N	5.801	19.850	131.651	102.546	68.891
T-L	5.818	15.750	51.926	64.504	26.315

temperature of 30-45°C in the gas state. At this time, the controller must ensure that the output follows the changed SP well. To check the SP tracking performance of the proposed controllers, a test of changing the SP to 40°C while the output temperature is maintained at 38°C was conducted and the result was compared with those of the other methods.

Fig. 11 shows that the proposed methods give better performances in terms of both swiftness and closeness of responses. The response of the Z-N method is the poorest, whereas the Seraji method shows a long rise time. For quantitative comparison, the rise time $t_r = t_{90} - t_{10}$, peak time t_p, overshoot M_p, 2% settling time t_s, and the integral of absolute error (IAE) were calculated and listed in Table 3. It can be clearly seen that the proposed methods exhibit smaller overshoot and reduced rise time and settling time than the other methods.

5.2. Response to disturbance changes

Once the warming-up process finishes, an operator no longer changes the SP and sets the controller to running mode. After that, the role of the controller is to make the output temperature return to the SP as quickly as possible whenever there is a disturbance. While the system is operating at 40°C, a simulation of changing the temperature of glycol returning to the heat exchanger from 30°C to 35°C is performed. Fig. 12 shows the responses. Fig. 12 shows that the proposed methods provide more improved performances as compared to the other methods.

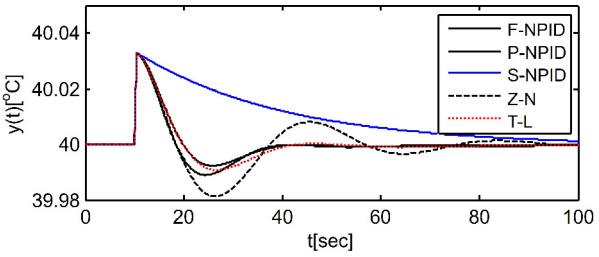

Fig. 12. Responses when a step-type disturbance is applied ($d = 30 \rightarrow 35$°C).

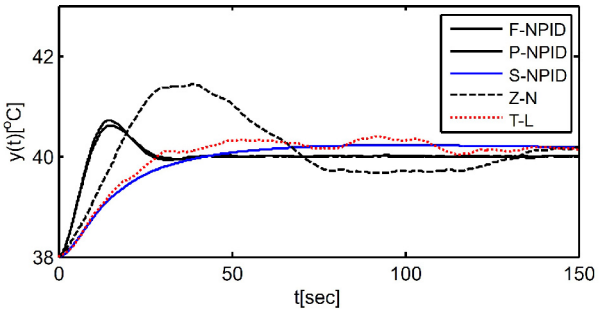

Fig. 13. Responses of the four methods when the SP is step-wisely changed from 35 to 40°C with Gaussian noise $\mathrm{N}(0, 0.01^2)$.

5.3. Response to noise rejection

A simulation was carried out to verify the performance of the proposed controllers in the presence of noise. It was assumed that there were noises in the range of -1.2-1.2°C when the outlet temperature of glycol was measured through a sensor. Fig. 13 shows that the proposed methods have a little change in responses, but the responses of the other methods are severely distorted due to the ideal derivative action.

5.4. Response to parameter changes

Next, the sensitivity of the system to parameter changes was verified. It was assumed that the gain K_h and time constant T_h of the heat exchanger change most severely. A simulation of increasing and decreasing these values by around 10% of the nominal value was performed (see Figs. 14-15). It is shown in the Figures that the proposed methods are less sensitive to the parameter changes than the other methods.

6. CONCLUSIONS

In this study, the two NPID controllers were proposed to control the outlet temperature of glycol by throttling a diaphragm valve installed in the LNG regasification system. A nonlinear function implemented by the T-S fuzzy model plays the role of continuously scaling the error of

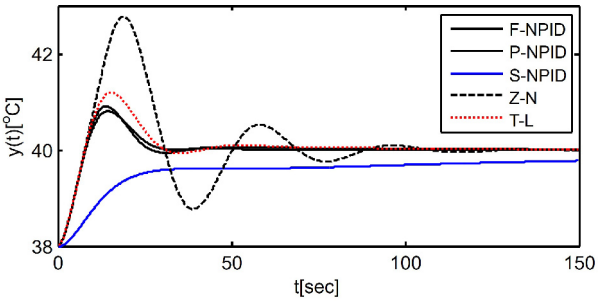

Fig. 14. Response comparison to parameter changes ($K_h = 12.5 \rightarrow 13.75$, $T_h = 30 \rightarrow 33$) while $y_r = 35 \rightarrow 40$°C.

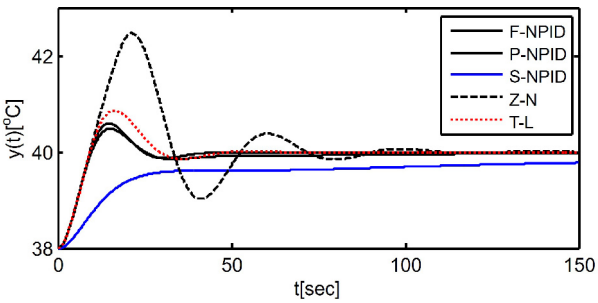

Fig. 15. Response comparison to parameter changes ($K_h = 12.5 \rightarrow 11.25$, $T_h = 30 \rightarrow 27$) while $y_r = 35 \rightarrow 40$°C.

as an input of the P, I, D actions so that the proposed controller can maintain satisfactory control performance despite environmental changes.

The controller parameters were tuned using a RCGA. To validate the proposed methods, the set-point tracking performance, less sensitivity to noise and parameter changes, and disturbance rejection performance were measured. Furthermore, the circle criterion was utilized to analyze the absolute stability of the nonlinear feedback system. The simulation results showed that the proposed controllers outperformed all the other methods and the performances of the F-NPID controller are slightly better than those of the P-NPID controller. However, in the case of the F-NPID controller, two more parameters than the conventional PID controller and one more parameter that P-NPID controller may be a burden for tuning and the maximum range of k_2 for absolute stability is slightly lowered to 1.783, while that of the F-NPID controller is 3.922. It could be seen that the P-NPID controller was more effective in terms of implementation, tuning and stability at the expense of the performance.

REFERENCES

[1] S. Kumar, H. Kwon, K. H. Choi, W. Lim, J. H. Cho, K. J. Tak, and L. L. Moon *et al.*, "LNG: An eco-friendly cryo-

genic fuel for sustainable development," *Applied Energy*, vol. 88, no. 12, pp. 4264-4273, December 2011.

[2] IMO, *Green House Gas Emissions from Ships*, Phase 1 Report, 2008.

[3] MAN Diesel & Turbo, *ME-GI Duel Fuel MAN B&W engines: A Technical, Operational and Cost-effective Solution for Ships Fuelled by Gas*, 2012.

[4] S. Jafarzadeh, N. Paltrinieri, I. B. Utne, and H. Ellingsen, "LNG-fuelled fishing vessels: A systems engineering approach," *Transportation Research Part D*, vol. 50, pp. 202-222, January 2017.

[5] V. Vinaya Krishna, K. Ramkumar, and V. Alagesan, "Control of heat exchangers using model predictive controller," *Proc. of IEEE Int. Conf. on Advances In Engineering, Science And Management*, pp. 242-246, March 2012.

[6] M. Pandey, K. Ramkumar, and V. Alagesan, "Design of fuzzy logic controller for a cross flow shell and tube heat-exchanger," *Proc. of IEEE Int. Conf. on Advances In Engineering, Science And Management*, pp. 150-154, March 2012.

[7] P. Sivakumar, D. Prabhakaran, and T. Kannadasan, "Temperature control of shell and tube heat exchanger by using intelligent controllers-case study," *Int. J. of Computational Engineering Research*, vol. 2, no. 8, pp. 285-291, December 2012.

[8] G. M. Sarabeevi and M. L. Beebi, "Temperature control of shell and tube heat exchanger system using internal model controllers," *Proc. of Int. Conf. on Next Generation Intelligent Systems (ICNGIS)*, February 2016.

[9] M. Korkmaz, O. Aydogdu, and H. Dogan, "Design and performance comparison of variable parameter nonlinear PID controller and genetic algorithm based PID controller," *Proc. of 2012 IEEE Int. Symp. on Innovations in Intelligent Systems and Applications*, pp. 1-5, July 2012.

[10] B. M. Isayed and M. A. Hawwa, "A nonlinear PID control scheme for hard disk drive servo systems," *Proc. of Mediterranean Conf. on Control & Automation*, pp. 1-6, June 2007.

[11] H. Seraji, "A new class of nonlinear PID controllers," *Proc. of 5th IFAC Robot Control*, pp. 65-71, September 1997.

[12] G. Zaidner, S. Korotkin, E. Shteimberg, A. Ellenbogen, M. Arad, and Y. Cohen, "Nonlinear PID and its application in process control," *Proc. of IEEE 26th Convention of Electrical and Electronics Engineers*, pp. 574-577, November 2010.

[13] H. Afrianto, M. R. Tanshen, B. Munkhbayar, U. T. Suryo, H. S. Chung, and H. M. Jeong, "A numerical investigation on LNG flow and heat transfer characteristic in heat exchanger," *Int. J. of Heat and Mass Transfer*, vol. 68, pp. 110-118, January 2014.

[14] A. O'Dwyer, *Handbook of PI and PID Controller Tuning Rules*, 2nd ed., Imperial College Press, London, 2006.

[15] T. Takagi and M. Sugeno, "Fuzzy identification of systems and its application to modeling and control," *IEEE Trans. Sys. Man and Cyber.*, vol. 15, no. 1, pp. 116–132, January 1985.

[16] H. K. Khalil, *Nonlinear Systems*, 3rd ed., Prentice Hall, New Jersey, 2002.

[17] Z. Michalewicz, *Genetic Algorithms + Data Structures = Evolution Programs*, Springer-Verlag, NY., 1992.

Gun-Baek So received his B.S degree in Marine Engineering and M.S degree in Control and Instrumentation Engineering from Korea Maritime and Ocean University, Busan, Korea, in 2009 and 2014, respectively. He is currently pursuing a Ph.D. at the Ocean Science and Technology School, Korea Maritime and Ocean University. His research interests include nonlinear control and genetic algorithms.

Hyun-Sik Yi received his B.S., M.S., and Ph.D. degrees, in Control and Instrumentation Engineering from Korea Maritime and Ocean University, Busan, Korea, in 1996, 1998 and 2001, respectively. His research interests include fuzzy control and modelling, process control, and genetic algorithms.

Yung-Deug Son received his B.S. degree in Control and Instrumentation Engineering from Korea Maritime University in 1997, an M.S. degree in Electro-Mechanical from Kobe University of Mercantile Ocean, Japan in 2001 and a Ph.D. degree in Electrical Engineering from Pusan National University, Korea in 2015, respectively. From 2001 to 2009, he was a Senior Research Engineer with Hyundai Heavy Industries Co., Ltd. Currently, he is an assistant professor at the Korea University of Technology and Education. His research interests include power conversion, electric machine drives, electrical facilities and renewable power system.

Gang-Gyoo Jin received his B.S. degree in Marine Engineering from Korea Maritime University, Busan, Korea in 1977, an M.S. degree in Electrical, Electronic and Computer Engineering, Florida Institute of Technology, USA in 1985, and a Ph.D. degree in Electrical, Electronic and Systems Engineering, University of Wales Cardiff, United Kingdom in 1996. Currently, he is a professor at the University of Maritime and Ocean University. His research interests include intelligent control, genetic algorithms and fractal.